ChemComm

COMMUNICATION

View Article Online
View Journal | View Issue

Cite this: *Chem. Commun.*, 2019, **55**, 14119

Received 5th September 2019,
Accepted 29th October 2019

DOI: 10.1039/c9cc06934h

rsc.li/chemcomm

pH clock instructed transient supramolecular peptide amphiphile and its vesicular assembly†

Payel Dowari,‡ Saurav Das,‡ Bapan Pramanik and Debapratim Das*

A new strategy to construct a transient supramolecular peptide amphiphile (SPA) and its vesicular aggregates is displayed. The construction of the amphiphile is assisted by the ternary complexation of cucurbit[8]uril and pH responsive imine bond formation. The transient assembly follows a pH clock set by urea/urease and hydrolysis of glucono delta-lactone (GdL). The transient assembly can be repeated for several cycles through feeding the system with the fuel (urea).

Self-assembly of simple molecules into complex and highly ordered systems that perform vital biological processes has been one of the principal tools used by nature for the creation as well as sustenance of life.[1] Most supramolecular systems are under thermodynamic control and the self-assembly process is generally an energetically down-hill process in which the stability of the assembled state is conferred by the formation of a low-energy equilibrium state.[2–4] However, many self-assembly processes occurring in nature such as the reversible formation of actin filaments,[5] formation of microtubules,[6] cell division,[6] motility[7] and signal transduction[8] are energetically demanding processes and require a constant influx of energy in order to retain the functional self-assembled state. The thermodynamic pathway of assembly is inadequate to maintain the functional efficacy of these systems and therefore such systems are kinetically driven where the assembly process is governed by the assembly pathway rather than the stability of the assembled state.[9] Such out of equilibrium self-assembly processes which are self-regulatory in nature and generate supramolecular assemblies of short finite lifetimes are referred to as transient self-assembly processes.

Recently, substantial efforts have been made to mimic the out of equilibrium processes in nature and to unravel the mysteries regarding the origin of life. The concept of transient assembly has been exploited to develop temporally controlled and short lived gels, vesicles, nano-reactors and nano-assemblies.[2,3,10–17] An elegant approach toward developing transient systems is to temporally control factors such as temperature, pressure, light, pH *etc.*[18,19] which mediate the formation of the self-assembled state. Using a combination of two competing triggers that induce a temporary change in pH from acidic to basic reaching a transient state before reverting back to the acidic range can be established.[20] Combining this pH clock efficiently with any self-assembling system whose assembly/disassembly is governed by the pH of the medium can lead to a transient self-assembled system.[3]

We anticipated that such a fuel-driven pH clock can be utilized to temporally form supramolecular peptide amphiphiles[21] and

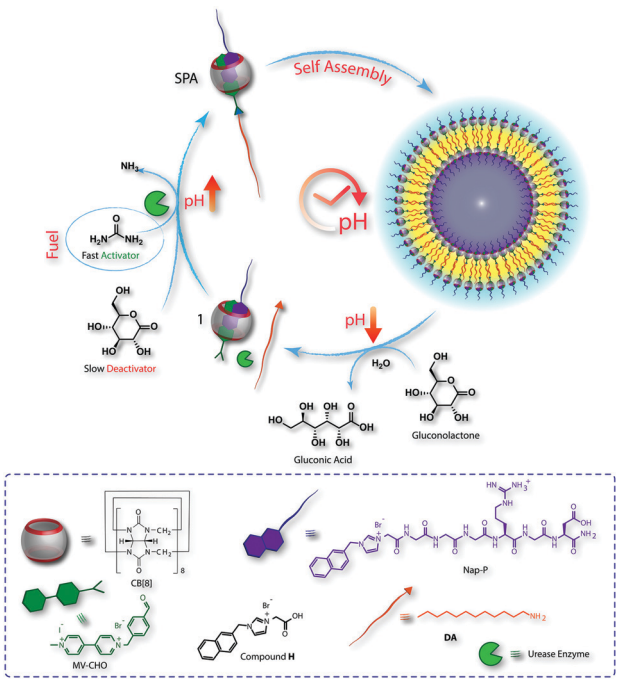

Scheme 1 Chemical structures of different components and graphical presentation of the pH clock driven temporal formation of a CB[8] assisted supramolecular peptide amphiphile and its vesicles.

Department of Chemistry, Indian Institute of Technology Guwahati, Assam 781039, India. E-mail: ddas@iitg.ac.in

† Electronic supplementary information (ESI) available: Experimental details, characterization data and other supporting figures. See DOI: 10.1039/c9cc06934h

‡ These authors contributed equally.

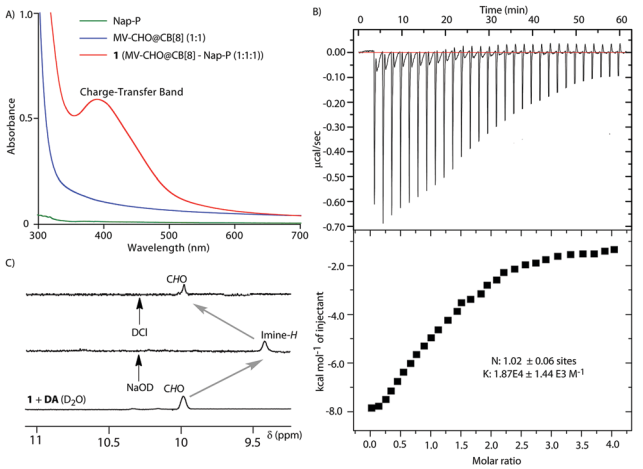

Fig. 1 (A) UV-Visible spectra of 0.75 mM aqueous solutions of different components of **1** showing the appearance of the charge transfer band upon ternary complexation in the case of **1**. (B) Thermograms (top) and binding isotherms (bottom) of MV-CHO@CB[8] with Nap-P at 298 K. (C) ^{1}H NMR of **1** and **DA** under different conditions showing the formation and disappearance of the SPA as a function of pH of the medium.

also their self-assembly. In this regard, cucurbit[8]uril (CB[8], Scheme 1)[22–24] assisted ternary complexation driven formation of supramolecular amphiphiles and their self-assembly into robust and stimuli responsive vesicles have been reported on several occassions.[25–28] Inspired by our previous experience with CB[8] based vesicles, herein we report pH regulated transient formation of a supramolecular peptide amphiphile (SPA) which self assembles to form transient vesicles.

Before constructing the pH clock and the transient system, the ternary complex (**1**) formation by a viologen unit (MV-CHO) and a naphthalene functionalized peptide (Nap-P) with CB[8] was confirmed by the appearance of the characteristic broad charge transfer (CT) band at 396 nm in the absorption spectra (Fig. 1A).[29] The isothermal titration calorimetric (ITC) experiment also showed a 1 : 1 complexation between Nap-P and MV-CHO@CB[8] (Fig. 1B).[30] Since a ^{1}H NMR experiment with Nap-P resulted in a complex spectrum, a shorter analogue, compound **H**, (Scheme 1) was used to understand the situation. The NMR spectra of different compositions of MV-CHO, **H** and CB[8] were recorded (Fig. S1, ESI†). The up-field shifts[31] of the MV- and naphthalene-protons of **H** in the presence of CB[8] disclose a slipped parallel stacking of the viologen and naphthalene units inside the CB[8] cavity (detailed explanation is provided in the ESI†). A similar slipped-stacking between donor acceptor groups has already been reported.[32,33] An ITC experiment using these molecules also shows 1 : 1 : 1 ternary complexation (Fig. S2, ESI†).

In the presence of dodecylamine (**DA**), the ternary complex **1** formed the desired SPA under basic conditions. The formation of the SPA was confirmed by the disappearance of the aldehyde signal and appearance of the imine peaks in the ^{1}H NMR spectra as shown in Fig. 1C. Imine bonds are dynamic covalent bonds (DCBs) which are stable at basic pH but are highly labile under acidic conditions.[34] The SPA breaks down to the parent amine and **1** upon acidification which is confirmed by the disappearance of the imine signals and re-appearance of the aldehyde proton. The formation–deformation of the SPA can thus be controlled using a pH switch.

To verify the proposed temporal aggregated system using this SPA, the pH clock was established. The pH clock (Scheme 1) has been realised by using a combination of two triggers: (i) the autocatalytic reaction of urea with the enzyme, urease, that releases NH_3 and leads to an increase in pH of the system, and (ii) the base-catalyzed saponification reaction of the dormant deactivator Glucono delta-lactone (GdL) as a counter trigger which furnishes gluconic acid and thereby decreases the pH. Upon addition of a mixture of urea and GdL in a definite ratio to an aqueous solution of the urease enzyme, initially a swift increase in pH was observed. After the activation kinetics of urease reaches its peak, no further rise in pH takes place. Under alkaline conditions, the hydrolysis of GdL is aggravated and initially, there is a rapid fall in pH until the pH reaches around 7.5 when the decrease in pH becomes slow and steady (Fig. 2A). A probable reason for this is that as the optimum pH for urease is 7.4,[35] the rate of formation of ammonia abruptly increases in this pH range and slows down the drop in pH. An increase in the concentration of urea and/or urease not only elevates the rate of activation but also causes an increment in the maximum overall pH. A high concentration of GdL restricts the rise in pH and escalates the rate of fall in pH. By fine tuning the rates of the activation and deactivation steps, the lifetime of the transient supramolecular assemblies can be easily modulated. An aqueous solution containing 0.2 mg mL^{-1} of urease showed an initial pH in the range of 6.5–6.8. The pH of the solution was adjusted to $\sim$5 before initiating the pH cycle. A very slow deactivation kinetics was observed when the amount of GdL was $\leq$2 equivalents of urea (Fig. 2A). This may be ascribed to the fact that one molecule of urea releases two molecules of NH_3, which neutralize the acid generated by GdL and thereby

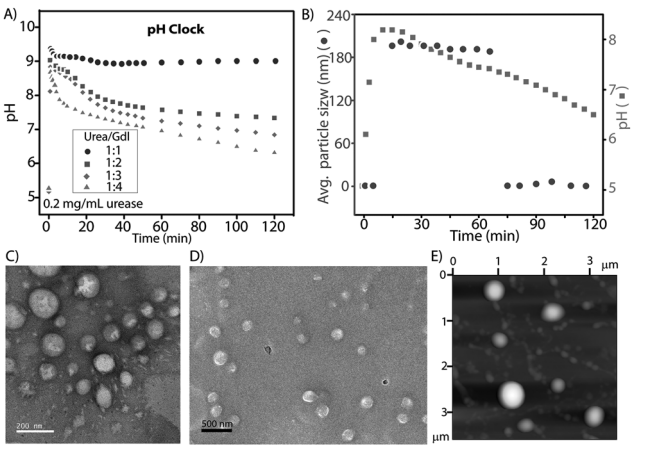

Fig. 2 (A) Optimizing the pH clock. The change in pH with time for four different urea/GdL compositions. (B) Appearance of particles of different sizes (from DLS) as a function of time for the transient system constructed by **1** and **DA** in the presence of 0.2 mg mL^{-1} urease, and 1 : 3 urea/GdL showing the response toward the pH clock. (C) FETEM, (D) FESEM and (E) AFM images of the transient vesicles formed during the cycle mentioned in (B).

slow down the decay in pH. In order to accelerate the deactivation step, the amount of GdL used should be sufficient to counter the neutralization caused by urea. Upon adding a mixture of urea and GdL in the ratio 1 : 3, an initial pH jump to 9.2–9.3 followed by a steady decay to 6.8–6.9 was observed in 120 minutes (Fig. 2A).

The kinetics of the transient formation of the SPA was then assessed under the influence of the pH clock. A 0.1 mM solution of the ternary complex, **1**, in water containing 0.2 mg mL^{-1} of urease and an equivalent amount (0.1 mM) of **DA** (dissolved in THF to facilitate solubilisation) showed an initial pH of 7.0–7.2. The presence of the amine might be responsible for this higher initial pH. The pH of the solution was adjusted to ~5 in order to avoid any SPA formation. The pH jump induced by the addition of urea and GdL (1 : 3) led to the transient generation of the SPA by the formation of imine bonds under alkaline pH conditions.

The aggregation process of the so formed SPA was monitored using Dynamic Light Scattering (DLS) measurements. Fig. 2B shows the appearance of particles of different sizes and change in pH of the system as a function of time. Prior to the addition of the triggers, no particular size distribution was observed in the DLS profile. However, aggregates with a hydrodynamic diameter of ~220 nm started (Fig. S3, ESI†) appearing soon after the pH clock started (addition of urea/GdL). Peaks corresponding to 220 nm distribution continued appearing until the pH of the system remained above 7.4 (~60 min). However, after that, the distribution disappeared completely. Even though the pH jump takes place almost instantaneously, aggregation takes place in a relatively slower and delayed fashion. This might be due to the reason that the ammonium ions present in the system might compete with **DA** for imine formation.[3] However, **DA**, owing to its stronger hydrophobic interactions in the assembled state, forms stronger imine bonds and outweighs the effect of ammonium ions. The aggregation pattern clearly demonstrates a pH dependent behaviour.

In order to determine the morphology of the supramolecular aggregates, microscopic techniques were employed. The FETEM image of the sample at pH 7.8 shows hollow spherical aggregates with a thin dark boundary which is indicative of the formation of vesicles (Fig. 2C). The diameter of the vesicles was found to be 200 nm which is in good agreement with the DLS data obtained. Furthermore, the absence of any specific morphology for the samples at pH below 7.4 corroborates the transient formation of vesicles. FESEM and AFM experiments also showed the formation of spherical aggregates with similar dimensions (Fig. 2D and E).

Ternary complexation induced formation of supramolecular amphiphiles and their vesicles are already demonstrated by our group and in the present case, the microscopic images also indicate the formation of vesicles.[27] However, it is important to confirm that the spherical aggregates are indeed vesicles. To prove the vesicular nature of the aggregates, diphenylhexatriene (DPH) was used which is well-known for the enhancement of emission upon encapsulation in the lipid bi-layer of vesicles.[2] In the present case, when the pH of the system (**1** + **DA**) is increased to ~8 by the addition of NaOH solution, significant enhancement in the emission (at 438 nm; λ_{ex} = 355 nm) was

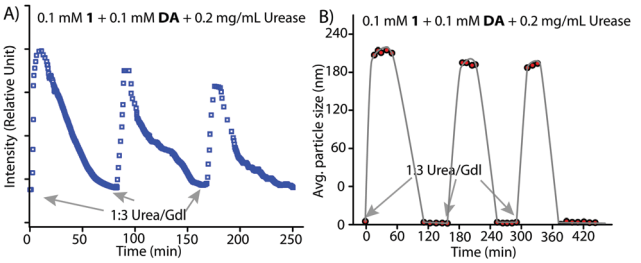

Fig. 3 Three consecutive cycles of the transient SPA and its vesicle formation as monitored by (A) emission spectra of DPH and (B) appearance of particles of different sizes as a function of time (from DLS).

observed which confirms the vesicular nature of the system (Fig. S4, ESI†). Upon addition of HCl to this system, the emission returns back to its original position. Furthermore, to confirm the transient nature, similar experiments were performed (**1** + **DA** + DPH + urease) in the presence of GdL-urea and a prominent enhancement in the emission of DPH was observed until 5 min followed by a decay to its original position within 90 min (Fig. 3A).

It is worth mentioning that, control experiments in the absence of CB[8] showed the formation of imine bonds at higher pH. However, neither any size distribution nor any particular morphology could be found for this system. The attachment of **DA** with MV-CHO certainly created an amphiphile which presumably could not form any vesicular aggregate as no particular morphology could be seen from microscopic experiments. Experiments with DPH also showed no change in the emission of the dye upon increasing the pH from 5 to 8 confirming the absence of vesicles (data not shown). It is well-established that asymmetric viologen amphiphiles are not capable of forming a vesicular assembly alone but ternary complexation with CB[8] assists the aggregation to vesicles.[36]

Confocal laser scanning microscopy (CLSM) was performed to directly visualize the assembly as well as the disassembly processes. A hydrophobic dye, Nile red (NR) was used to facilitate the visualization of the aggregates. A control experiment with **1** and **DA** at pH 8 showed vesicle like structures under the microscope (Fig. S5, ESI†). The fluorescent spots remained unchanged for 2 h ensuring no photo-bleaching. During the experiment under the pH clock, initially, no fluorescence was observed in the absence of pH triggers due to the absence of any vesicles (Fig. 4). However, the fluorescence intensity of NR increased abruptly after 15 minutes due to the addition of the fuel indicating the formation of vesicles and entrapment of NR. As the reaction proceeds further, the fluorescence intensity diminishes slowly indicating the breakdown of the vesicles. One cycle of vesicle formation and dissociation was visualized by recording an image every 30 s. Time lapsed movies for one such cycle have been provided as Videos S1 and S2 (ESI†). The number of fluorescent objects (Fig. S6, ESI†) was then counted to quantify the analyses. From the movies, Fig. 4 and Fig. S6 (ESI†), the formation and dissociation of the vesicles is clearly visible as the number of fluorescent particles increased and then disappeared following the pH clock.

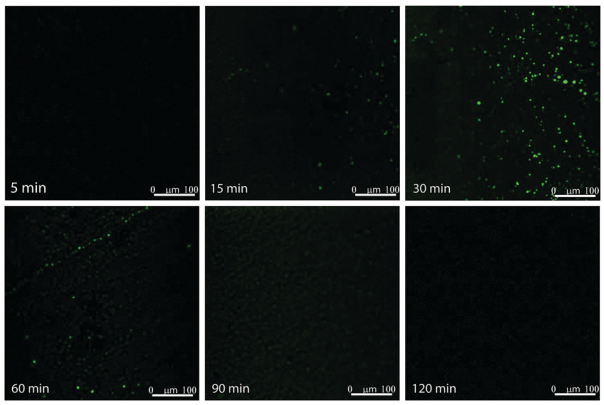

Fig. 4 CLSM images of the transient system constructed by **1**, **DA**, 0.2 mg mL^{-1} urease, and 1 : 3 urea/GdL in the presence of NR at different times showing the temporal formation of the vesicles.

Having established the transient formation of vesicles, we were interested to check the repeatability of the transient assembly by refuelling after each cycle. Refuelling after the first cycle reproduced similar cycles of events and the aggregation in subsequent cycles was studied using DLS and fluorescence spectroscopy (using DPH) as shown in Fig. 3A and B. In subsequent cycles, a lower rise in initial pH followed by a rapid decay in pH was observed (Fig. S7, ESI†). The DLS data also showed a steady decrease in the lifetime of the assembled state in consecutive cycles. This fall in efficiency of the pH clock is due to the accumulation of gluconic acid in the system after each cycle which increases the overall acidity of the system. Fluorescence studies using DPH as the hydrophobic probe also showed an increase in the fluorescence intensity followed by a steady decay. The second reaction cycle shows a nearly identical variation in the fluorescence intensity which indicates the stability of the system under repeated pH cycles.

To gain further insight into the dynamics of the aggregation, DLS studies were performed with aliphatic amines of varying chain lengths (Fig. S8, ESI†). The chain length had no significant effect on the aggregation behaviour and time scale. However, a direct proportionality between the size of the aggregates and the chain lengths could be observed as the average diameter increases with the chain length of the amine.

In conclusion, we have shown the transient formation of a SPA which subsequently forms a vesicular assembly in response to a pH clock. The formation of the SPA is assisted by the ternary complexation by CB[8]. The pH clock is established by combining urea/urease based fast biocatalytic processes and slow hydrolysis of GdL. The imine bond formation under basic conditions and its hydrolysis under an acidic medium are the key chemical transformations used for the construction of the SPA and its transient assembly. The temporal formation of the vesicle requires chemical fuel to maintain the out-of-equilibrium state and several cycles of the transient assembly can be achieved by supplying the fuel to the system.

DD acknowledges financial support from SERB (EMR/2016/000857), India, and the UKIERI (DST/INT/UK/P-119/2016), India.

Conflicts of interest

There are no conflicts to declare.

Notes and references

1 D. J. Kushner, *Bacteriol. Rev.*, 1969, **33**, 302–345.
2 S. Maiti, I. Fortunati, C. Ferrante, P. Scrimin and L. J. Prins, *Nat. Chem.*, 2016, **8**, 725.
3 A. Jain, S. Dhiman, A. Dhayani, P. K. Vemula and S. J. George, *Nat. Commun.*, 2019, **10**, 450.
4 J. Wang, K. Liu, R. Xing and X. Yan, *Chem. Soc. Rev.*, 2016, **45**, 5589–5604.
5 E. Reisler and E. H. Egelman, *J. Biol. Chem.*, 2007, **282**, 36133–36137.
6 A. Desai and T. J. Mitchison, *Annu. Rev. Cell Dev. Biol.*, 1997, **13**, 83–117.
7 A. J. Howard and R. R. L. Clark, *Appl. Mech. Rev.*, 2002, **55**, B39–B39.
8 S. O. Rizzoli, *EMBO J.*, 2014, **33**, 788–822.
9 E. Mattia and S. Otto, *Nat. Nanotechnol.*, 2015, **10**, 111.
10 S. De and R. Klajn, *Adv. Mater.*, 2018, **30**, 1706750.
11 M. Kumar, N. L. Ing, V. Narang, N. K. Wijerathne, A. I. Hochbaum and R. V. Ulijn, *Nat. Chem.*, 2018, **10**, 696–703.
12 S. Bal, K. Das, S. Ahmed and D. Das, *Angew. Chem., Int. Ed.*, 2019, **58**, 244–247.
13 H. Wang, Y. Wang, B. Shen, X. Liu and M. Lee, *J. Am. Chem. Soc.*, 2019, **141**, 4182–4185.
14 F. della Sala, W. Verbeet, S. Silvestrini, I. Fortunati, C. Ferrante and L. J. Prins, *ChemNanoMat*, 2018, **4**, 821–830.
15 J. Boekhoven, W. E. Hendriksen, G. J. M. Koper, R. Eelkema and J. H. van Esch, *Science*, 2015, **349**, 1075–1079.
16 J. P. Wojciechowski, A. D. Martin and P. Thordarson, *J. Am. Chem. Soc.*, 2018, **140**, 2869–2874.
17 G. Wang, B. Tang, Y. Liu, Q. Gao, Z. Wang and X. Zhang, *Chem. Sci.*, 2016, **7**, 1151–1155.
18 S. Panja, C. Patterson and D. J. Adams, *Macromol. Rapid Commun.*, 2019, **40**, 1900251.
19 P. K. Kundu, D. Samanta, R. Leizrowice, B. Margulis, H. Zhao, M. Börner, T. Udayabhaskararao, D. Manna and R. Klajn, *Nat. Chem.*, 2015, **7**, 646.
20 T. Heuser, A.-K. Steppert, C. M. Lopez, B. Zhu and A. Walther, *Nano Lett.*, 2015, **15**, 2213–2219.
21 A. Dasgupta and D. Das, *Langmuir*, 2019, **35**, 10704–10724.
22 K. I. Assaf and W. M. Nau, *Chem. Soc. Rev.*, 2015, **44**, 394–418.
23 S. K. Steven, J. Barrow, M. J. Rowland, J. del Barrio and O. A. Scherman, *Chem. Rev.*, 2015, **115**, 12320–12406.
24 D. Das, K. Assaf and W. Nau, *Front. Chem.*, 2019, **7**, 619.
25 Y. J. Jeon, P. K. Bharadwaj, S. Choi, J. W. Lee and K. Kim, *Angew. Chem., Int. Ed.*, 2002, **41**, 4474–4476.
26 D. Jiao, J. Geng, X. J. Loh, D. Das, T.-C. Lee and O. A. Scherman, *Angew. Chem., Int. Ed.*, 2012, **51**, 9633–9637.
27 J. H. Mondal, S. Ahmed, T. Ghosh and D. Das, *Soft Matter*, 2015, **11**, 4912–4920.
28 J. H. Mondal, T. Ghosh, S. Ahmed and D. Das, *Langmuir*, 2014, **30**, 11528–11534.
29 Y. H. Ko, E. Kim, I. Hwang and K. Kim, *Chem. Commun.*, 2007, 1305–1315.
30 M. E. Bush, N. D. Bouley and A. R. Urbach, *J. Am. Chem. Soc.*, 2005, **127**, 14511–14517.
31 Y.-M. Zhang, J.-H. Liu, Q. Yu, X. Wen and Y. Liu, *Angew. Chem., Int. Ed.*, 2019, **58**, 10553–10557.
32 B. Pramanik, S. Ahmed, N. Singha, B. K. Das, P. Dowari and D. Das, *Langmuir*, 2019, **35**, 478–488.
33 N. Singha, B. K. Das, B. Pramanik, S. Das and D. Das, *Chem. Sci.*, 2019, DOI: 10.1039/C9SC03417J.
34 B. Pramanik and D. Das, *J. Phys. Chem. C*, 2018, **122**, 3655–3661.
35 S. D. Cesareo and S. R. Langton, *FEMS Microbiol. Lett.*, 1992, **99**, 15–21.
36 J. H. Mondal, S. Ahmed and D. Das, *Langmuir*, 2014, **30**, 8290–8299.

